A STUDY ON NON DESTRUCTIVE TESTS AND FLEXURAL STRENGTHS OF GEOPOLYMER CONCRETE USING COMBINATION OF DIFFERENT FINE AGGREGATES

M.Indhumathi[1], V.Ragavan[2], A.Dhanalakshmi[3], D.Darling Helen lydia[4]

[1,2,4]Civil Engineering Department,Ramco institute of Technology,Rajapalayam,India
[3]Civil Engineering PSR College of Engineering,India

Abstract: Geopolymer concrete is a new technology that deserves more attention in the rapidly evolving sustainable construction industry. Furthermore, to avoid the depletion of natural resources, by-product waste management technologies are essential. Today, river sand is in short supply. DMS (Dredged Marine Sand), on the other hand, which faces disposal and land acquisition issues, proves to be a viable alternative to river sand. In this paper, a mixture of M-Sand and DMS was used in place of river sand, and non-destructive, Flexural strength of beam by monotonic loading and cyclic loadings were investigated. The findings indicated that DMS has attained flexural characteristics and with regard to cracks, very minor and vertical cracks are observed in all beams as in the case of monotonic loading. Further, they originate from the tension zone

Keywords:Geopolymer concrete, Flexural Strength, DMS,M-sand,Non Destructive Tests.

1. Introduction

Joseph Davidovits (1989) conducted extensive research on the chemistry of geopolymers and geopolymeric materials. Geopolymer undergoes exothermic reactions as a result of the polycondensation process, as previously stated. The geopolymer materials are clearly stated to be derived from mineral earth resources. Composites are created without the use of fire, smoke, toxins, or excessive energy during the manufacturing process. The investigations conclusively demonstrated that geopolymeric materials immobilise harmful elemental wastes within the geopolymeric matrix. Hazardous components in flyash reacted with

---

1Correspondingauthor: *indhumathi@ritrjpm.ac.in*, *vragavan@ritrjpm.ac.in[2]* , *dhanalakshmicvl@psr.edu.in[3]*

geopolymer compounds to form the three-dimensional framework of the geopolymermatrix[1].

Malhotra (1990) evaluated the durability of structural concrete containing high quantities of low-calcium fly ash, which has been studied by CANMET since 1985. The inclusion of a large volume of air entrained flyash improved its performance in freezing and thawing cycles. Because of the low heat of hydration and the low cement concentration, it is ideal for use in huge buildings. It demonstrates that a large amount of flyash concrete is used in concrete building. It significantly lowers the expansion caused by the alkali silica reaction [2].

Rangan (2010)[3] published a research report on flyash-based geopolymer concrete that covered mix design, compressive strength, acid resistance, sulphate resistance, economic benefits, reinforced geopolymer concrete beams and columns, and curing technique. It was also mentioned that flyash-based geopolymer concrete is best suited for structural purposes. The structural behaviour and stress strain properties of flyash-based geopolymer concrete and Portland cement concrete were found to be identical. Furthermore, because of the low calcium content, geopolymer concrete has excellent acid resistance, low creep, limited sulphate attack, and drying shrinkage. Geopolymer concrete is cost-effective since it makes use of waste materials. In addition, the production of geopolymer concrete uses significantly less energy and emits no CO2.

PradipNath et al. (2015) investigated the early age properties of low-calcium flyash geopolymer concrete under ambient curing with GGBS[4]. Early age parameters such as settig time, workability, flow value, and compressive strength were studied. GGBS was discovered to have a significant influence on the early age characteristics. Furthermore, compressive strength increased as the percentage of binder material increased, including some additives. Various additives were tested, and GGBS was shown to be the best alternative for flyash in ambient curing circumstances.

Amin noushini et al. (2018) focussed on mechanical and flexural performance of synthetic fibre reinforced geopolymer concrete. Mechanical and flexural parameters were investigated on flyash based geopolymer concrete mixed with monofilament, fibrillated polypropylene fibre and polyolefine. Models were also formed using experimental data. Fibre reinforced geopolymer concrete consisting polypropylene fibre was found to have decrease in compressive strength at about 1%-7%. The reason behind the reduction in strength was mentioned as due to its low modulus of elasticity and also due to air pockets formed around the fibre. The given stress strain model clearly explained the post peak, stress strain behaviour, stress at peak etc for both plain and fibre reinforced geopolymer concrete (fly ash based). However a remarkable improvement was seen in flexural parameters (flexural toughness)to about 1.5-2.5 times when fibrillated polypropylene fibres were used. Fracture energy also got increased due to the usage of polyolefin fibres admixed with geopolymer concrete.

Wei liu et al. (2016) investigated the carbonation of Dredged Marine Sand concrete and its effect on chloride binding. DMS's physical and chemical properties were investigated at the microstructure level. It was possible to monitor the behaviour of DMS chloride in concrete and concrete carbonation. The physical adsorption of chloride ions into free chloride ions is clearly induced by the disintegration of C-S-H gel. CO_2 diffusion rates may be lowered by increasing the ratio of capillary holes. Steel bar corrosion in concrete can be decreased by utilising DMS concrete, which has a better carbonation resistance. Concrete carbonation increased in DMS due to free chloride ions.[5],[6].

Chu S.H. and Yao J.J. (2020) created a concrete strength model using marine dredging sediments. Strength prediction was explored in both qualitative and quantitative modes. The volume of marine dredging sediment, paste volume, water volume, cement volume, and so

on were recognised as critical elements influencing strength.[7] For more generic applications, a prediction equation based on the data of 112 blends was developed. The study shed new light on in-situ concrete synthesis using dredged marine sediments.[8]

Juntao Dang et al. (2020) investigated the hydration, strength, and microstructure of mortar made from discarded marine clay. The effect of calcination temperature, particle fineness, and cement replacement ratio on the pozzolanic activity of thermally treated marine clay was investigated. It was determined that including 15% fine calcined marine clay as a cement substitute gives the needed strength in comparison to the reference mortar.[9]

According to the above-mentioned literature survey, several studies on constituent materials utilised in geopolymer concrete, such as fly ash, GGBS, M-Sand, and DMS, have already been conducted. Mechanical properties, microstructure analysis, fracture parameters, durability issues, and corrosion research on geopolymer concrete have also been studied. Work on geopolymer mortars and concretes has also been described. However, research on mixing M-Sand and DMS with flyash-GGBS under ambient curing conditions is restricted. This finding is based on a thorough literature review as well as a prior art search (exploring the world's published patent/application/non-patent literature). The prior art search revealed that the earlier works are highly relevant prior artto the current inquiry is zero, closely relevant prior art is one, relevant prior art is four, and fascinating references are eleven. The UNO score (on a scale of 10) obtained for the current inquiry in terms of industrial applicability is 8, novelty is 7, inventive step is 7, and overall score is 7.3. As a result, the current work, which aims to investigate the flexural strength and non-destructive tests on fly ash-based geopolymer concrete using M-Sand and DMS under ambient curing conditions, would be a work aiming to suggest alternative fine aggregates for Geopolymer Concrete that would also facilitate ambient curing conditions.

2. Experimental Research

2.1 Materials:

In addition to GGBS, Class F fly ash is employed as a binder to aid in the polymerization process. As previously stated, GGBS is used to achieve ambient curing conditions.

Alkaline solutions, 98% pure sodium hydroxide (NaOH) and A53 grade sodium silicate, were produced 24 hours before casting the specimens. Though a combination of potassium alkaline liquids can be explored, sodium alkaline liquids are recommended from an economic standpoint.

In place of typical fine aggregate, a mixture of M-sand and DMS in varied proportions is utilised. IS 383-2016 specifies M-sand (Zone II) and DMS (Zone I).

According to the mix design, coarse aggregates in the sizes of 7mm, 14mm, and 20mm were used from neighbouring quarries.

Polypropylene fibres with densities of 910kg/m3, lengths of 19mm, nominal diameters of 55m, thicknesses of 0.2 mm, Young's modulus of 3500N/mm2, and aspect ratios of 345.5 were employed.To improve workability,

Master Glenium Sky 8233 super plasticizer is applied. The amount added is approximately 1% of the total volume of geopolymer concrete.

2.2 Mix Design and Test Methods:

As per Rangan and Hardjito methodspecimens of size 100X100X500mm and 150mmX200mmX1500mm were cast for investigating flexural parameters..D100 (100 percent DMS), M100 (100 percent M-Sand) and R100 (100 percent conventional river sand) mixes were used having flyash and GGBS percentages as constant (Flyash-70%, GGBS-30%)

3. Experimental Investigation

3.1 Flexural Strength of PRISM

To determine flexural strength of geopolymer concrete in a small scale manner, prism specimens of size 100mm x100mm x500 mm (Figure.3.1) were cast . Specimens were tested in loading frame of capacity 1000 kN (Figure.3.2). Testing was done as per IS 516-1959 norms. Two point loading in the direction of length of prisms was adopted.

Figure 3.1 Prism specimens

Figure 3.2 Loading frame set up

3.2 Flexural Strength of Beams
3.2.1 Monotonic loading

To determine flexural strength in a large scale manner,reinforced geopolymer concrete beams of size 150mm x 200mm x1500mm were cast as shown in Figure 4.11. Measures were taken to prevent localised buckling during fabrication. Clear cover to reinforcement (25mm) was also ensured. Reinforcement was designed as per IS: 456-2000 for an effective span of 1300mm. 3-10Y were provided at the bottom of the beam as per design. 8Y bars at 100mm c/c at shear span and 200mm c/c in pure bending area were provided as shear reinforcement. Based on the results of mechanical properties, beams were cast for D40, D100, M100 and R100 proportions. Needle vibration was done to ensure good compaction. Monotonic load was applied as shown in Figure 3.3. Two point loading was adopted. The load was gradually applied on the beam at the rate of 5 kN per step. The load cell sensitivity was fixed as 0.1kN.The load was transferred through the spreader beam of I section. Two LVDT were fixed under the loading point system to record the deflection. Data acquisition system was used for the investigation.
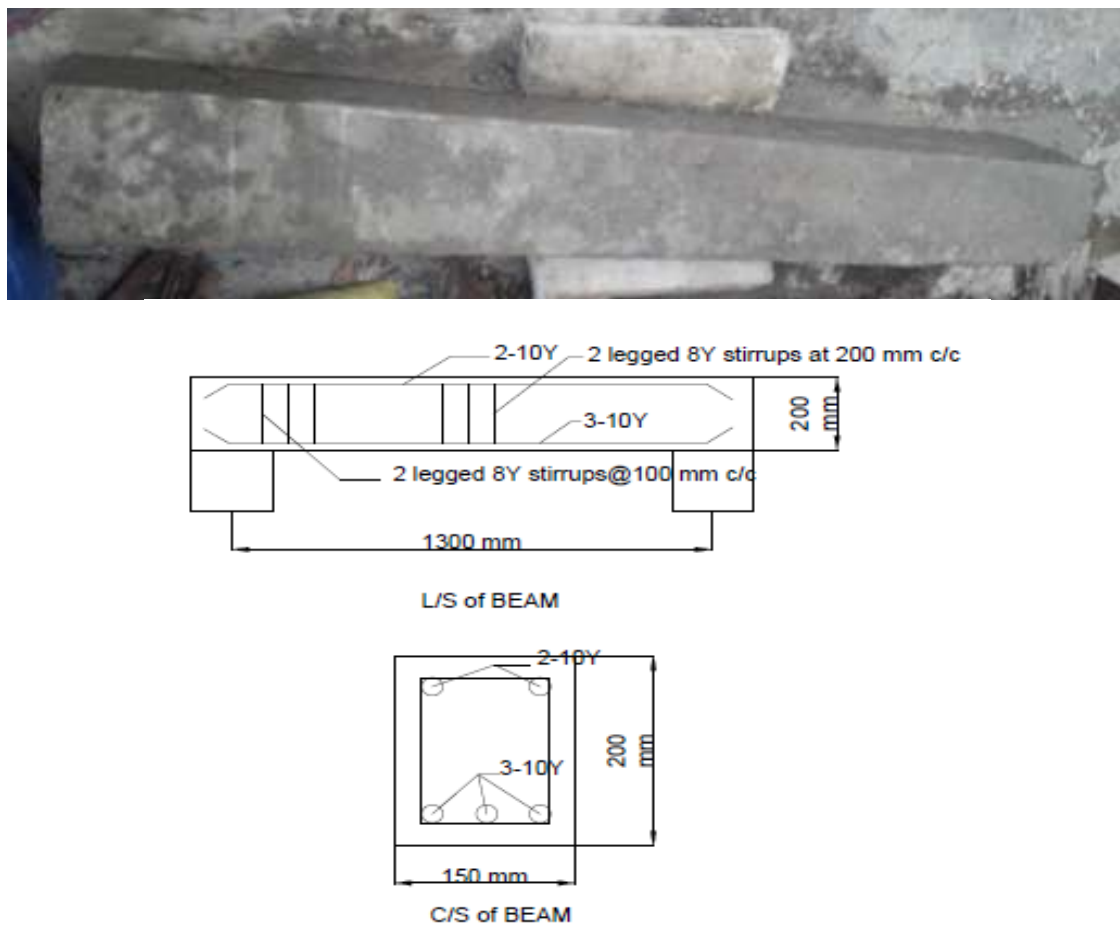
Figure 3.3 Cast beam for monotonic loading

Figure 3.4 Test setup for beam test

3.2.2   Cyclic loading

The beams cast for the purpose of applying cyclic loading had a section of 150mm x 200 mm x 1500 mm as shown in Figure 3.5. 10 Y bars were used for main reinforcement as well for hangar bars. 6mm diameter bars were used for stirrups. The beam was designed as under reinforced section for an effective span of 1300mm. Needle vibrator was used for compaction. Clear cover of 25mm was maintained on all sides. Hydraulic servo controlled loading frame of 100kN capacity was used for testing as shown in Fig 3.6. Actuators were used for the purpose. For cyclic loading case, D100, R100 and M100 proportion specimens were used. Loading was applied from 0 to 15kN, then 0 to 30kN, 0 to 45kN, 0 to 60kN, 0 to 75kN and 0 to 90kN. Loading rate was fixed as

0.01kN/sec(YonglaiZheng and Isamu Yoshitake, 2020). Corresponding deflection of each and every increment of load cycles were recorded. The first crack load was also noted and yield load, ultimate load, energy absorption, ductility index and stiffness values were arrived.

Figure 3.5 Cast specimen for cyclic loading

Figure 3.6 Test setup for cyclic loading

3.3   Non Destructive Testing

To have additional evidence on strength values obtained in destructive tests, non destructive testing was also done by ultrasonic pulse velocity test as well by rebound hammer method of testing.

3.3.1   Ultra sonic pulse velocity test

Ultrasonic pulse velocity technique for determining the quality of hardened concrete has been done as per the procedure specified in IS: 13311 (Part 1) – 1992. The time taken for the ultrasonic pulse velocity to pass through hardened concrete specimens was observed. The test set up will be as shown in Figure 4.15. The equipment consists of two parts namely a pulse generator capable of generating waves and a pulse receiver to receive the waves. The inbuilt shock-exciting piezo-electric crystals serve the purpose of generating and receiving waves.

Table 3.1 shows the quality of concrete with regard to the calculated pulse velocity.

Table 3.1 Pulse velocity Vs Concrete quality

Pulse velocity (km/second)	Concrete Quality (Grading)

Above 4.5	Excellent
3.5 to 4.5	Good
3.0 to 3.5	Medium
Below 3.0	Doubtful

Following points were taken care during the test.
1. To avoid errors arising out of heterogeneity of concrete, the minimum path length should be kept as 30 cm
2. Temperature conditions influence the pulse velocity.
3. Pulse path was chosen carefully to avoid the influence of reinforcing steel on the pulse velocity.

Figure 3.7 Ultrasonic pulse velocity test

3.3.2   Rebound hammer test

The procedure outlined in IS 13311 (Part-2): 1992 was followed for carrying out the rebound hammer test on specimens. Rebound hammer consists of a mass controlled by spring which slides on a plunger within a tubular housing. The compressive strength of concrete could be assessed by the relation between rebound index and compressive strength. Rebound hammer method can very well be used for identifying the questionable and acceptable parts of a structure.

The hammer was forced against the concrete surface and the rebound distance was measured on a scale. (Figure 3.8)

Figure 3.8 Rebound hammer test

3.4   Stress Strain Characteristics

Stress strain curve of concrete represents graphically the concrete behaviour under applied load. This was obtained by testing cylinder specimens of size 150mm x 300mm in compression testing machine as shown in Figure 3.9. The curve was obtained (IS:456-2000)by plotting concrete compressive strain at various intervals of concrete compressive loading (stress)

The performance of structures can also be very well be monitored by studying the stress strain characteristics. Further, the nature of failure can be obtained by this.

Figure 3.9 Compressive stress strain

## 4. RESULTS AND DISCUSSIONS

4.1   FLEXURAL STRENGTH

Prisms of size 100 mm x 100 mm x 500 mm were cast to determine the flexural strength. Loading rate of 180 kg/ min was fixed throughout the experiment. The obtained flexural strength values are tabulated in Table 4.1.

Table 4.1 Flexural strength results

S. No.	Mix ID	Flexural strength (Mpa)
		28 Days
1.	D20	7.530
2.	D40	6.636
3.	D60	6.322
4.	D80	6.585
5.	D100	7.823
6.	M100	8.004
7.	R100	8.123

The variation of flexural strength of prisms are shown in Figure 4.1.
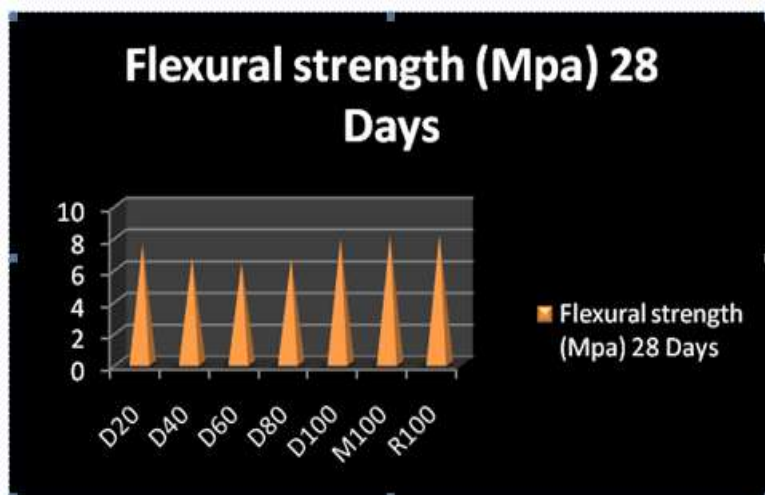
Figure 4.1 Flexural strength

From Figure 4.1, it shall be seen that the variation of flexural strength also followed same pattern as that of compressive strength and split tensile strength. Initially, the values got decreased and started increasing from D80 specimens proceeding to still higher values at D100. As such, it shows that geopolymer concrete produced using DMS behaves well in flexure too.

4.2   FLEXURAL STRENGTH OF REINFORCED GEOPOLYMER CONCRETE

4.2.1   Deflection Behaviour of Geopolymer RC Beam Under Monotonic Load

The load-deformation behaviour ofreinforced geopolymer concrete beams of identity D40, D100, M100 and R100 were studied for pure bending case by subjecting to four point bending test. The structural parameters namely first cracking load(P_{cr}),yield load (P_y) and ultimate load (P_u) were observed. The results obtained for D40 and D100 were compred with that of control mixes M100 and R100.

The load increments and corresponding deflection measured at mid span as well at $1/3^{rd}$ of span for D100 is given in Table 4.2.

Table 4.2 Load-deflection values for D100

Load	D100	
	Mid span	$1/3^{rd}$ span
2.02	0.00	0.00
5.34	0.49	0.21
10.31	0.99	0.71
16.23	1.49	1.28
22.71	1.98	1.56
29.02	2.51	2.32
33.45	3.01	2.86
37.60	3.50	3.26
42.54	4.01	3.88
47.51	4.51	3.93
52.68	5.01	4.23
57.61	5.51	4.33
Table 4.2 Continued		

62.32	6.01	4.62
66.81	6.51	4.89
71.79	7.03	5.08
76.62	7.53	5.23
81.26	8.00	5.98
84.55	8.52	6.01
85.39	9.03	6.23
87.13	9.53	6.93
87.90	10.05	7.02
89.12	10.53	7.29
90.23	10.89	7.32

The load increments and corresponding deflection measured at mid span as well at $1/3^{rd}$ of span for D40 is given in Table 4.3.

Table 4.3 Load deflection values for D40

Load	D 40	
	Mid span	$1/3^{rd}$ span
2.82	0.00	0.00
4.80	0.50	0.22
7.19	1.03	0.74
9.05	1.51	1.28
10.94	2.03	1.56
12.99	2.52	2.32
15.10	3.02	2.86
17.21	3.53	3.26
19.16	4.03	3.88
21.37	4.53	3.93

Table 4.3 Continued

23.56	5.03	4.23
25.86	5.54	4.33
27.92	6.03	4.62
30.11	6.54	4.89
32.26	7.05	5.08
34.34	7.54	5.23
36.46	8.04	5.98
38.56	8.54	6.01
40.69	9.06	6.23
42.63	9.54	6.93
44.47	10.06	7.02
45.41	10.54	7.29
46.19	11.06	7.32
48.23	11.18	7.89
52.38	11.23	8.01
54.82	11.44	8.23
56.23	11.56	8.57
58.11	12.32	8.94
60.22	12.89	9.07
63.11	13.25	9.63

65.22	13.59	9.82
66.33	14.46	10.09
67.88	15.22	10.22
68.44	15.69	10.89
70.56	15.96	11.95
71.83	16.02	12.22

The load increments and corresponding deflection measured at mid span as well at 1/3rd of span for M100 is given in Table 4.4.

Table 4.4 Load-deflection values for M100

Load	M 100	
	Mid span	1/3rd span
2.66	0.00	0.00
6.82	0.48	0.33
12.64	1.00	0.69
18.67	1.47	1.36
25.53	1.99	1.65
31.31	2.49	2.23
36.22	3.01	2.56
41.09	3.51	3.18
45.89	4.00	3.98
51.02	4.51	3.99
56.27	5.01	4.21
61.73	5.51	4.43
67.38	6.02	4.71
72.37	6.51	4.85
77.78	7.01	5.11
83.22	7.50	5.25
85.22	7.68	5.57
86.38	7.89	5.69
87.19	7.98	5.97
88.29	8.02	6.07
90.86	8.26	6.18
91.15	8.53	6.23
92.56	8.69	6.39

The load increments and corresponding deflection measured at mid span as well at 1/3rd of span for D100 is given in Table 4.5.

Table 4.5 Load-deflection values for R100

Load	R 100	
	Mid span	1/3rd span
0.72	0.00	0.00
2.94	0.51	0.12
6.36	0.99	0.18
11.15	1.49	0.53
17.15	2.01	0.98
23.46	2.50	1.08
28.91	2.99	1.19

33.69	3.51	1.26
38.43	4.01	2.01
43.2	4.50	2.29
48.18	5.03	2.89
52.95	5.52	2.93
57.86	6.01	3.21
62.91	6.52	3.36
75.21	7.02	4.28
80.22	7.52	4.29
85.56	8.02	5.26
89.23	8.52	5.89
90.02	8.66	5.92
90.59	8.99	6.56
91.76	9.23	6.83
92.89	9.46	7.09
93.18	9.61	7.12

The load vs mid span deflection values are plotted as shown in Figure 4.5 and the failure loads, deflections, stiffness values and ductility parameters are given in Table 4.5
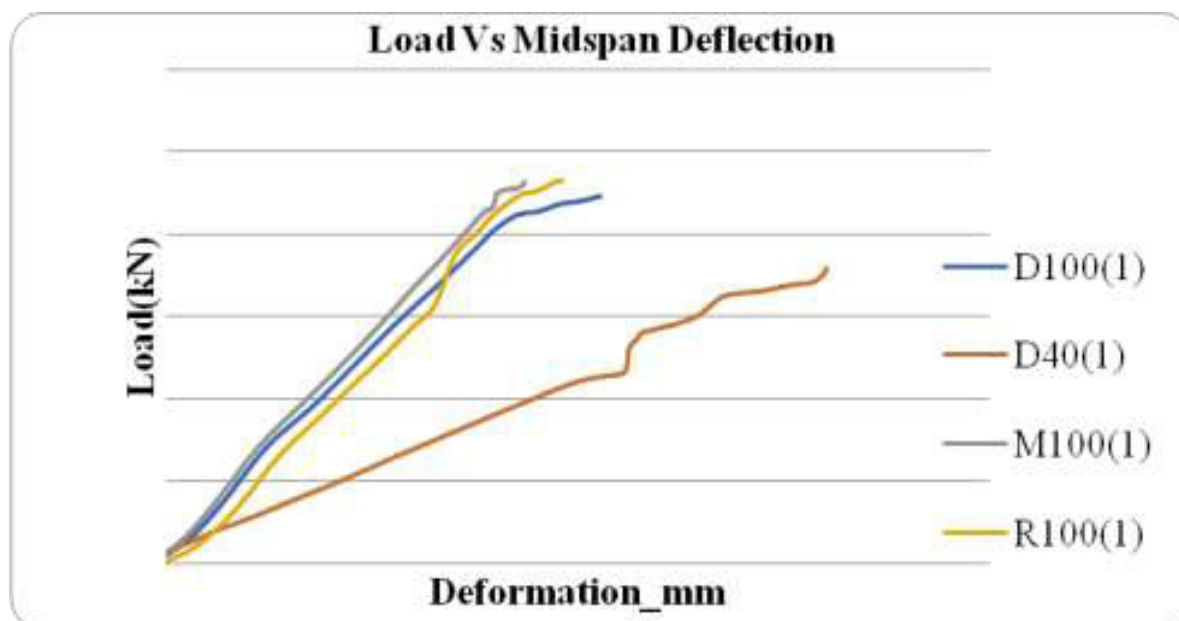
Figure 4.5 Load Vs Midspan deflection

Table 4.5   Failure loads, deflections, stiffness values and ductility parameters

Mix Id	Load (kN)		Deflection (mm)		Initial stiffness (kN/mm)	Ultimate stiffness (kN/mm)	Energy ductility Index (P_u/P_x)	Displacement ductility index(Δ_u/Δ_x)
	Yield P_x	Ultimate P_u	Yield Δ_x	Ultimate Δ_u				
D100	84.55	90.23	8.52	10.89	9.92	8.28	1.067	1.27
D40	46.19	71.83	11.06	16.02	4.17	4.48	1.55	1.44
M100	90.86	92.56	8.26	8.69	11	10.65	1.02	1.05
R100	75.21	93.28	7.02	9.61	10.71	9.70	1.24	1.37

The following observations were made from the load-deflection study carried out under monotonic loading:

(i) The formation of first crack is much delayed and also minimum number of cracks only in all mixes.

(ii) All observed cracks are minor and originate from tension zone of beam. (Figure 4.6 to Figure 4.9)

(iii) Load-deflection behaviour of D100 is found similar to that of control mixes M100 and R100.

(iv) Each mix has achieved the target strength of G40 and the maximum deflection of 16.02 mm in the case of D40.

(v) Minimum deflection in the case of M100 and corresponding load being 92.56kN.

(vi) The ultimate load carrying capacity is high for R100 while compared to others though other mixes are also having fairly nearer values except D40.

(vii.) Comparing D40 and D100, D100 carries greater load (90.23kN) with lesser deflection (10.89mm).

(viii.) While comparing control mixes M100 and R100, M100 showed good load-deflection behaviour.

(ix.) Initial stiffness as well ultimate stiffness values are also greater starting from M100, R100 and D100.

Figure 4.6 Tested D40 beam specimen

Figure 4.7 Tested D100 beam specimen

Figure 4.8 Tested M100 beam specimen

Figure 4.9 Tested R 100 beam specimen

The observed deflection of all mixes at 1/3rd span are shown in Figure 4.10.

Figure 4.10 Load Vs 1/3rddeflection

Load Vs 1/3rd deflection curves also yield the same inference as above.

4.3   Stress Strain Behaviour of Beam

The stress-strain behaviour obtained for all the mixes D40, D100, M100 and R100 are shown in Figure.4.11. The stress-strain behaviour of control specimens M100 and R100 are almost similar. Compared to D100, D40 specimens have undergone much strain for the given loading.
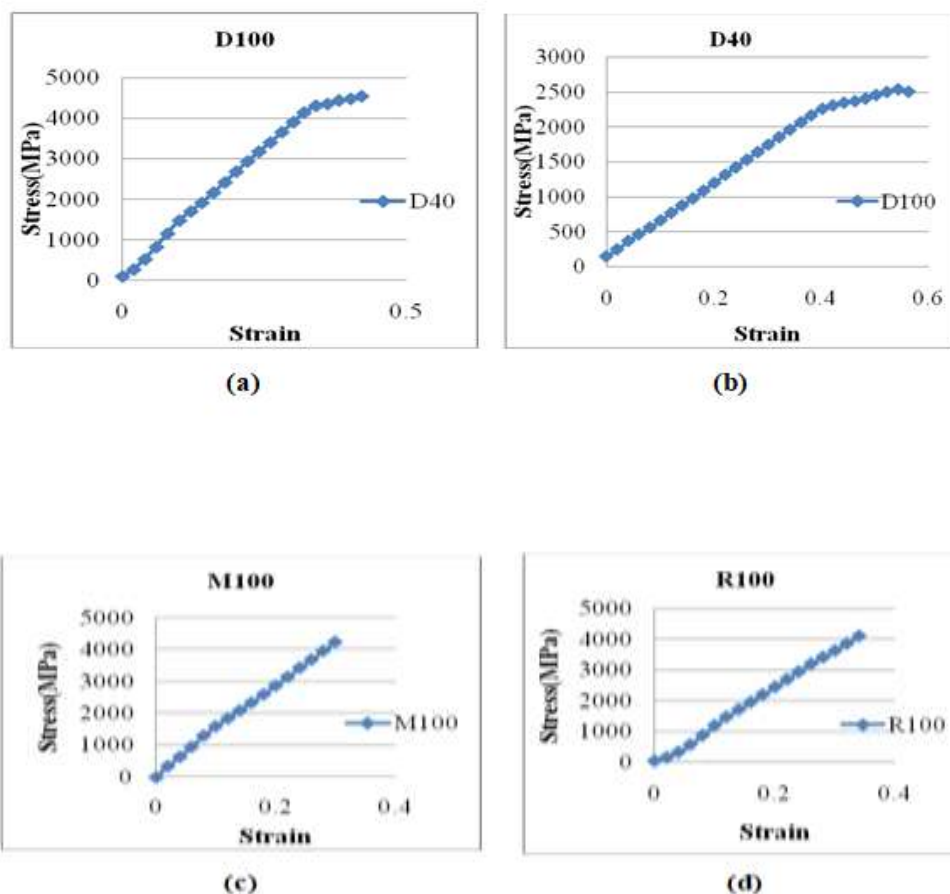
Figure 4.11 Stress-strain (a) D100, (b) D40, (c) M100 and (d) R100

4.4   Behaviour of Geopolymer RC Beam Under Cyclic Loading

Cyclic loading behaviour was made with an objective to monitor response of geopolymer RC beams to dynamic loads especially when structures are subjected to vibration and earthquake load. Totally 3 no of beams were cast to investigate the cyclic behaviour of RC beams namely for mixes D100, R100 and M100. Loading was givenas (0-15-0)kN,   (0-30-0)kN,   (0-45-0)kN, (0-60-0)kN   and   (0-75-0)kN   as   shown   in   the   loading   history   diagram (Figure 4.12).
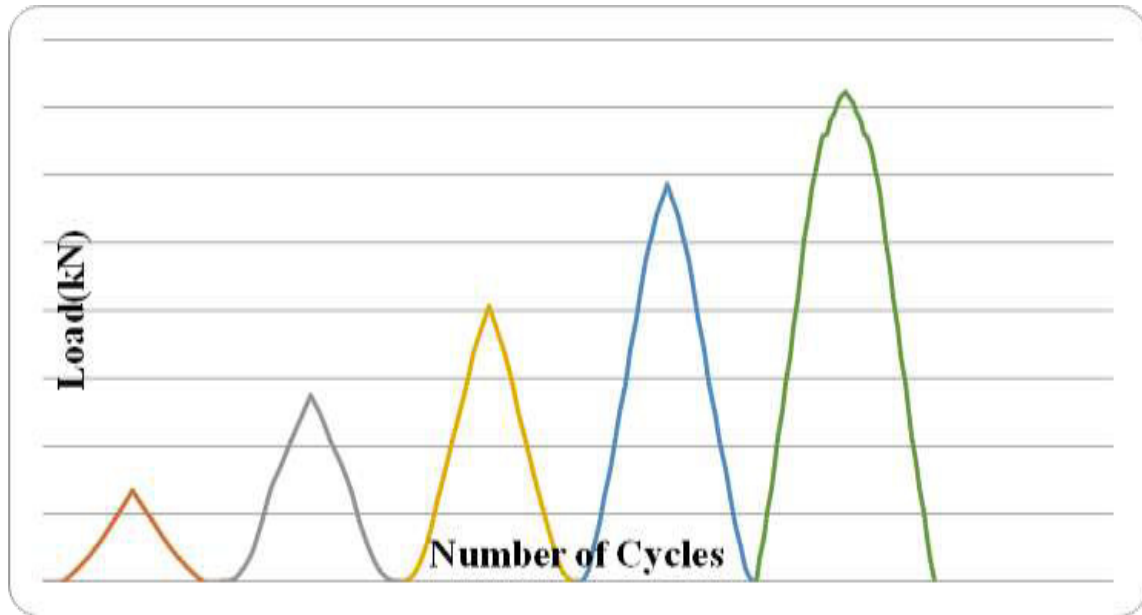
Figure 4.12 Loading history of cyclic loading

The factors observed during the study of cyclic load behaviour are
  i)   Load deflection curve
  ii)   Load carrying capacity

The observation made is given in Table.4.6

Table 4.6 Results of cyclic loading

Mix Id	Deflection (mm)		Yield load(kN)	First crack load(kN)	Ultimate load for cyclic loading (kN)
	Yield	Ultimate			
D100	3.36	18.23	11.28	32.85	65.27
M100	2.98	16.26	14.19	41.22	80.26
R100	2.11	13.97	18.91	45.36	85.23

The specimens after cyclic loading are shown in Figure 4.13 to Figure 4.15

Figure 4.13 D100 beam after cyclic loading

Figure 4.14 M100 beam after cyclic loading

Figure 4.15 R100 beam after cyclic loading

The load-deformation characteristics of specimens subjected to cyclic loading are shown in Figure 4.16 to Figure 4.18.
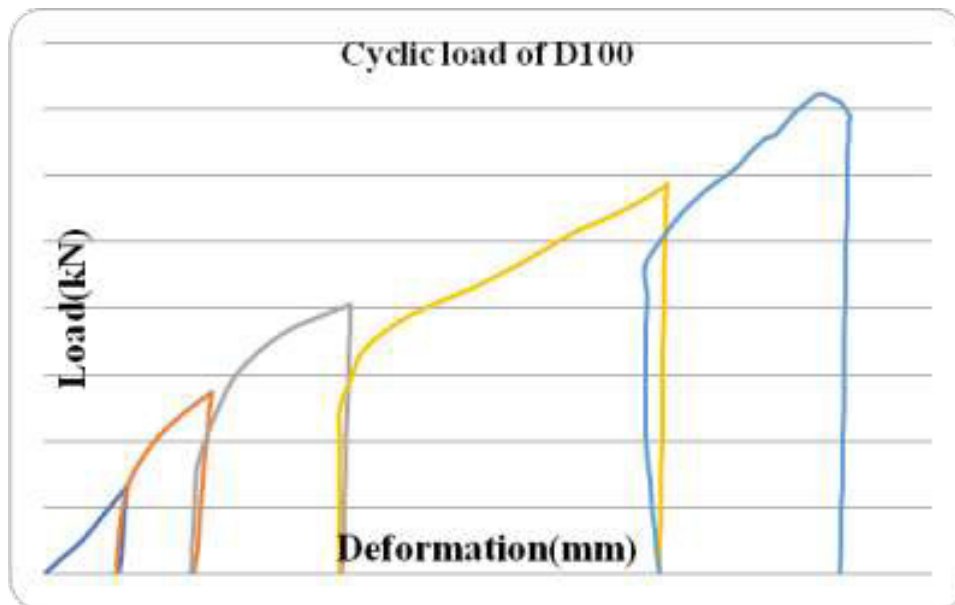
Figure 4.16 Load Vs Deformation - D100
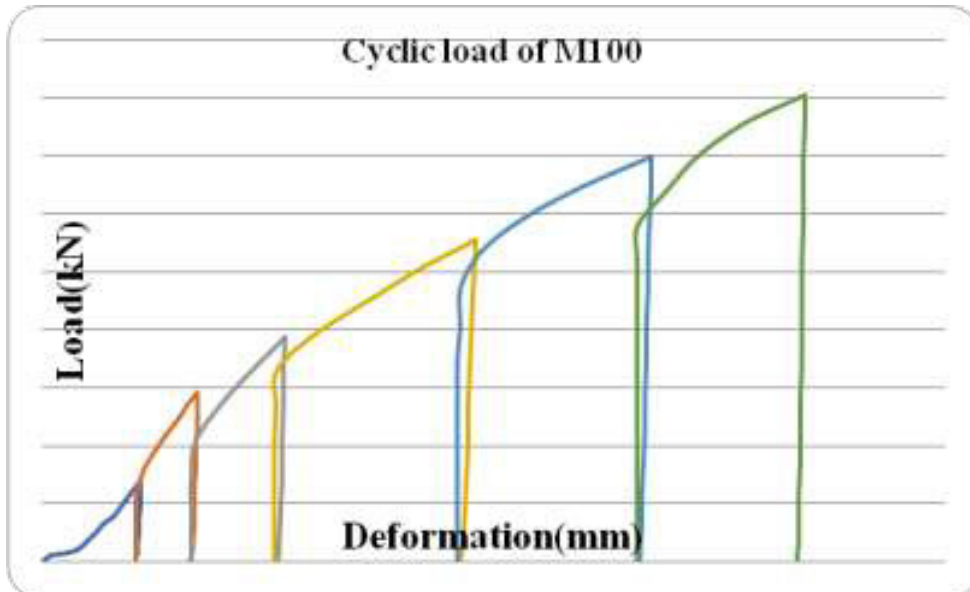
Figure 4.17 Load Vs Deformation - M100
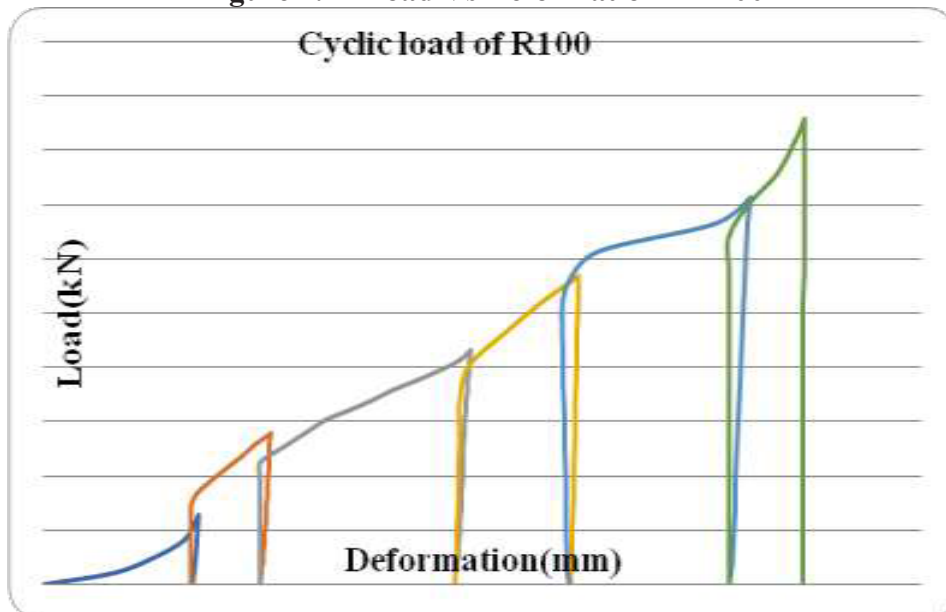
Figure 4.18 Load Vs Deformation - R100

From the load deflection curve, the following observations are made:

i) Compared to D100, M100 and R100 mixes, R100 shows good load-deflection characteristics.

ii) The ultimate load carrying capacity is more in R100 and compared to it, M100 and D100 experienced reduction in ultimate load of 5.8% and 23.46% respectively. Higher reduction in ultimate load in D100 specimen may be due to the reason of poor bonding characteristics of DMS with the binder and coarse aggregate when subjected to cyclic load.

iii) Compared to the deflection of D100 beam, M100 and R100 got deflection reduced by an amount of 10.8% and 23.36% respectively.

iv) With regard to cracks, very minor and vertical cracks are observed in all beams as in the case of monotonic loading. Further, they originate from the tension zone.

v) The ultimate load and corresponding deflection was less in cyclic loading when compared to that of monotonic loading.

The obtained load vs time graph during cyclic loading are shown in Figure 4.19 to Figure 4.21.
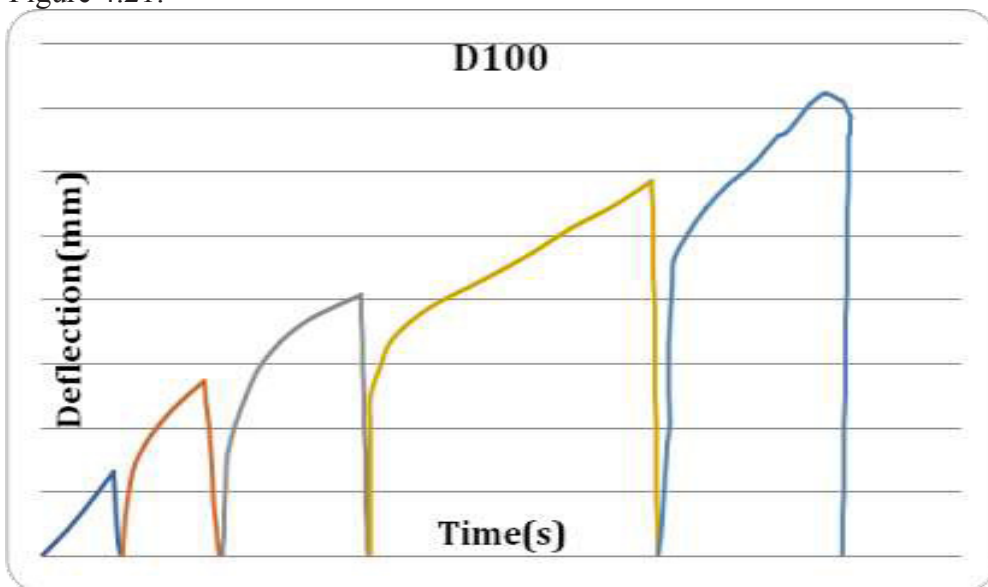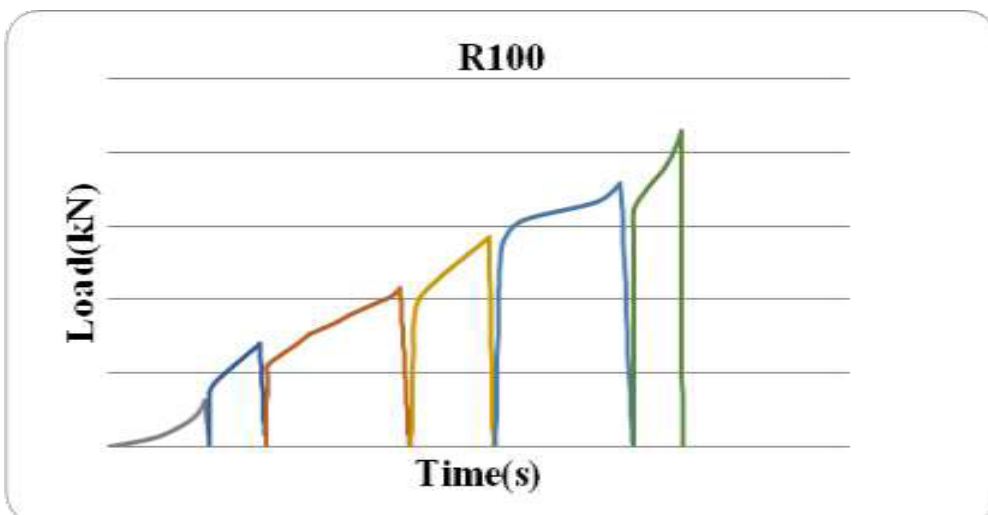
Figure 4.19 Load Vs Time - D100
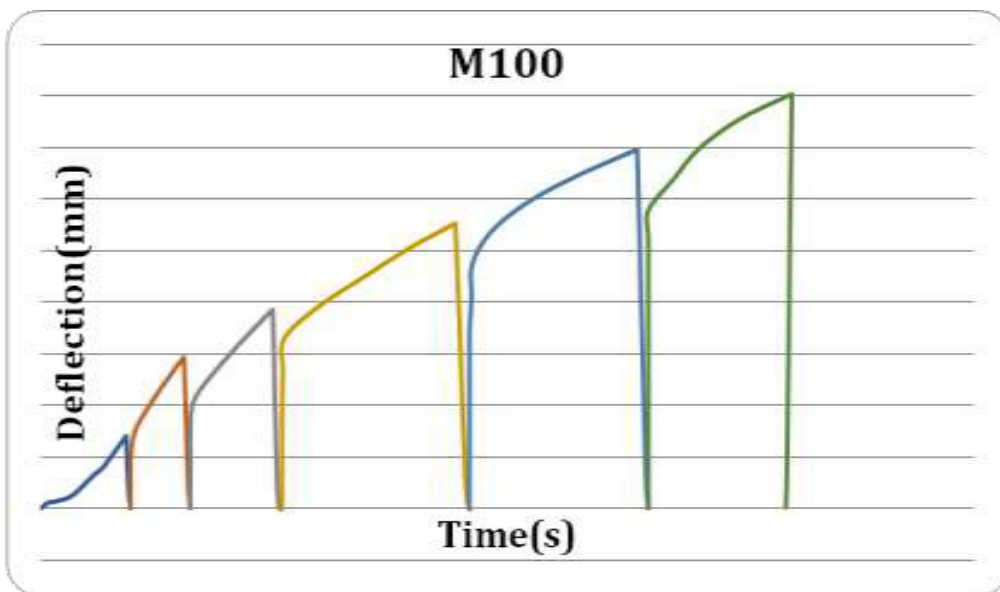
Figure 4.20 Load Vs Time for M100

Figure 4.21 Load Vs Time for R100

4.5   NON DESTRUCTIVE TESTING

The results obtained by rebound hammer test as well by ultrasonic pulse velocity test are discussed in this section.

4.5.1   Rebound Hammer Test

The hardness values obtained for all mix proportions from rebound hammer test are given in Table.4.7

Table 4.7 Rebound hammer test

S. No.	Mix ID	Hardness (Mpa)
1.	D20	47.09
2.	D40	46.78
3.	D60	37.26
4.	D80	39.21
5.	D100	48.22
6.	M100	50.86
7.	R100	52.09

The comparison of hardness values of different mixes is shown in Figure 4.22.
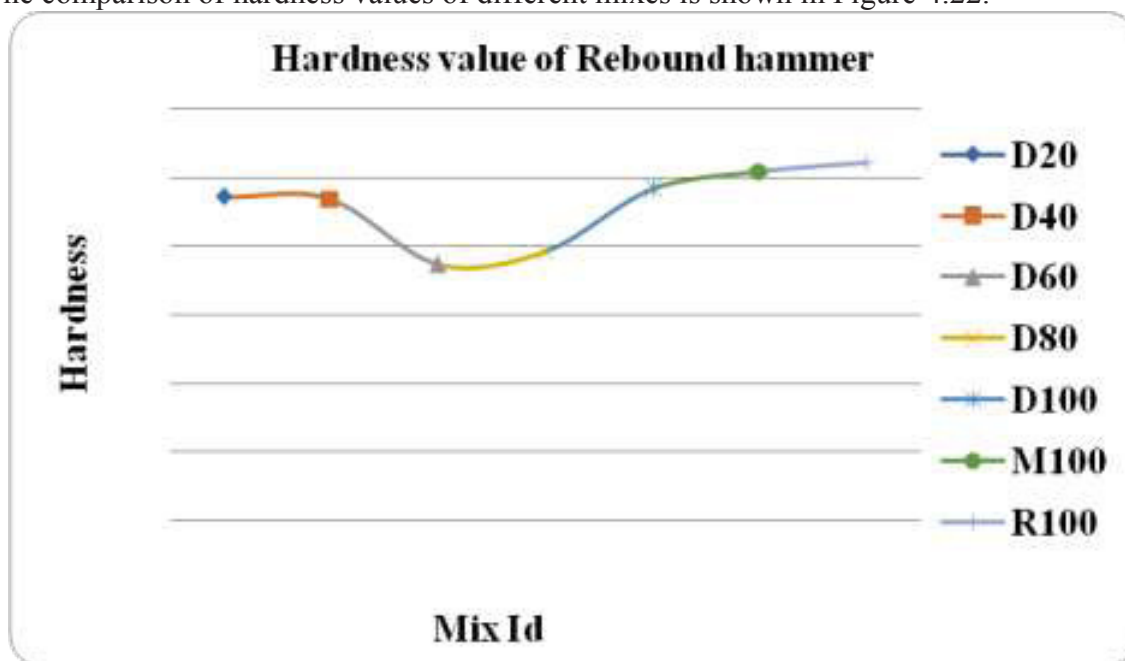
Figure 4.22 Comparison of hardness values

From Figure 4.22, it shall be seen that among DMS specimens, hardness value of D100 is greater. While comparing control mix specimens, R100 gave maximum value. In general, D100 behaves at par with M100 and R100 specimens. D20 gives fairly equal value as that of D100 giving an indication that 100% percent DMS gives good strength and if at all combination of aggregates is sought, 20 – 80 (DMS-M-Sand) and vive versa shall be preferred. From D40 to D60, strength gets reduced due to the reason stated earlier that insufficient cohesion existing betweeen the two different fine aggregages.
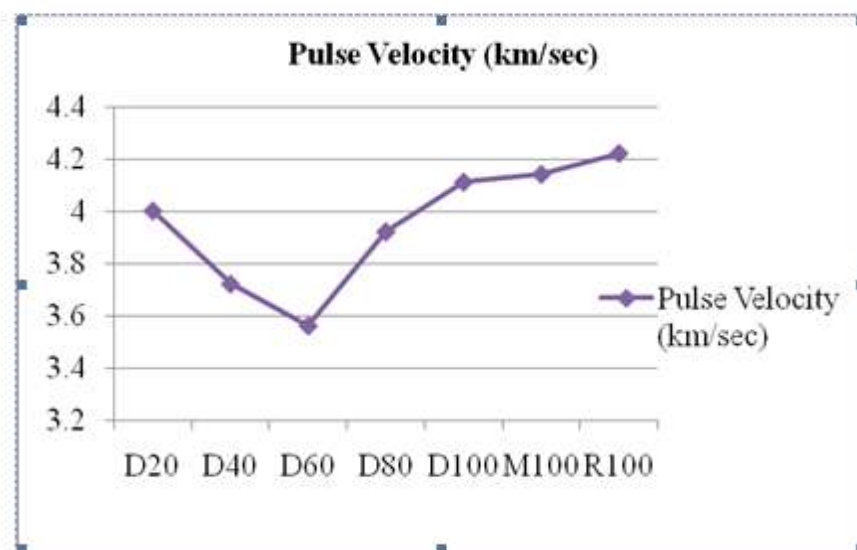
4.5.2   Ultrasonic Pulse Velocity Test

As a part of non destructive testing, ultrasonic pulse velocity test was also doneand the obtained results are given in Table 4.8.

Table 4.8 Ultra sonic pulse velocity results and inferred Quality

S. No.	Mix Identity	Time (µ Sec)	Distance travelled (m)	Pulse Velocity (km/sec)	Quality
1.	D20	37.5	0.15	4.00	Excellent
2.	D40	40.3	0.15	3.72	Good
3.	D60	42.1	0.15	3.56	Good
4.	D80	38.2	0.15	3.92	Good
5.	D100	36.5	0.15	4.11	Excellent
6.	M100	36.2	0.15	4.14	Excellent
7.	R100	35.5	0.15	4.22	Excellent

The ultrasonic pulse velocity obtained in the case of all mixes are shown in Figure 4.23.

Figure 4.23 Ultrasonic pulse velocity

From Figure.4.23, it shall be seen that maximum ultrasonic pulse velocity is obtained in the case of D100 among the DMS specimens reflecting well packed particles. The reduced pulse velocity in the case of D40 to D60 specimens reveal that voids exist between two different fine aggregates.

Thus, the inferences made in destructive tests match very well with that of non destructive tests.

### 4.5.3   STATISTICAL RESULTS

With the experimental results obtained on compressive strength, split tensile strength, flexural strength and the results of non-destructive testing, regression equations were developed.Regression analysis yielded nonlinear equations and coefficent of correlation (R^2). The equations developed and coefficent of correlation obtained are given in Table 4.9

Table 4.9 Regression analysis equations and coefficients

S. No.	Identification	Equation	Coefficient of correlation R^2
1.	Compressive strength Vs Split tensile strength	$y = 4.025x^2 - 5.356x + 29.56$	0.815
2.	Compressive strength Vs Flexural strength	$y = 4.069x^2 - 48.95x + 177.6$	0.889
3.	Compressive strength Vs Rebound hammer	$y = 0.113x^2 - 8.961x + 207.9$	0.821
4.	Compressive strength Vs Ultrasonic pulse velocity	$y = 34.17x^2 - 234.1x + 429.0$	0.935

From the above, it shall be seen that R^2 values vary from 0.80 to 0.94 indicating that difference between the experimental values and estimated values is not much.

The regression plots are shown in Figure 4.24 to Figure 4.27.
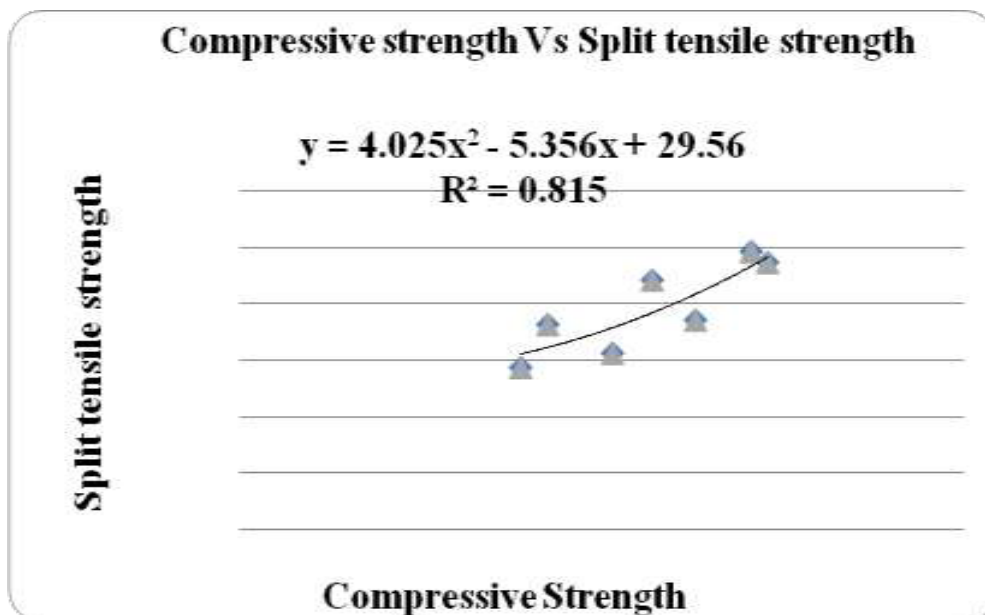
Figure 4.24 Compressive strength Vs Split tensile strength

Compressive strength Vs Flexural strength

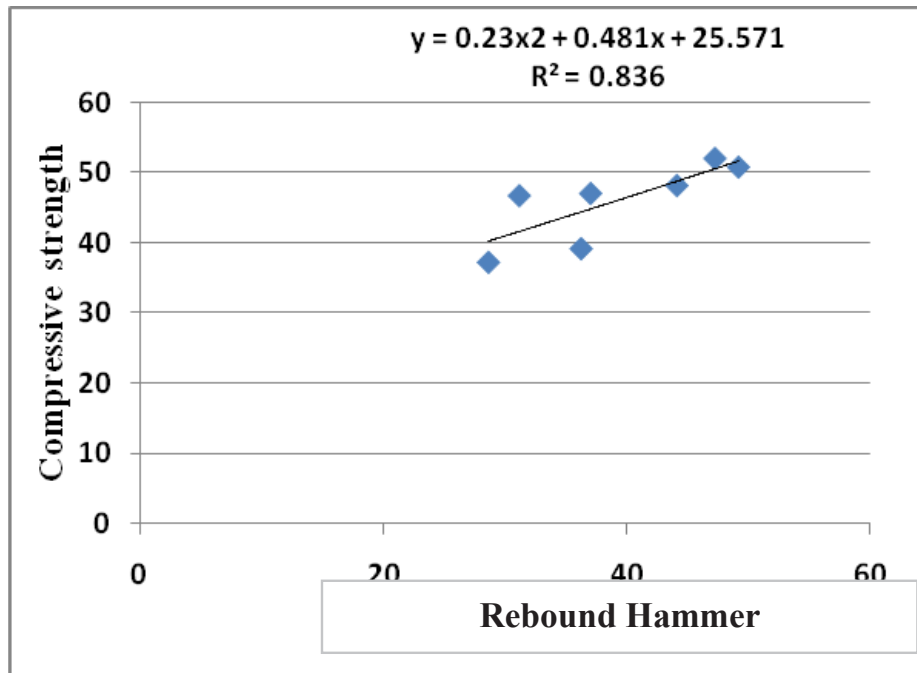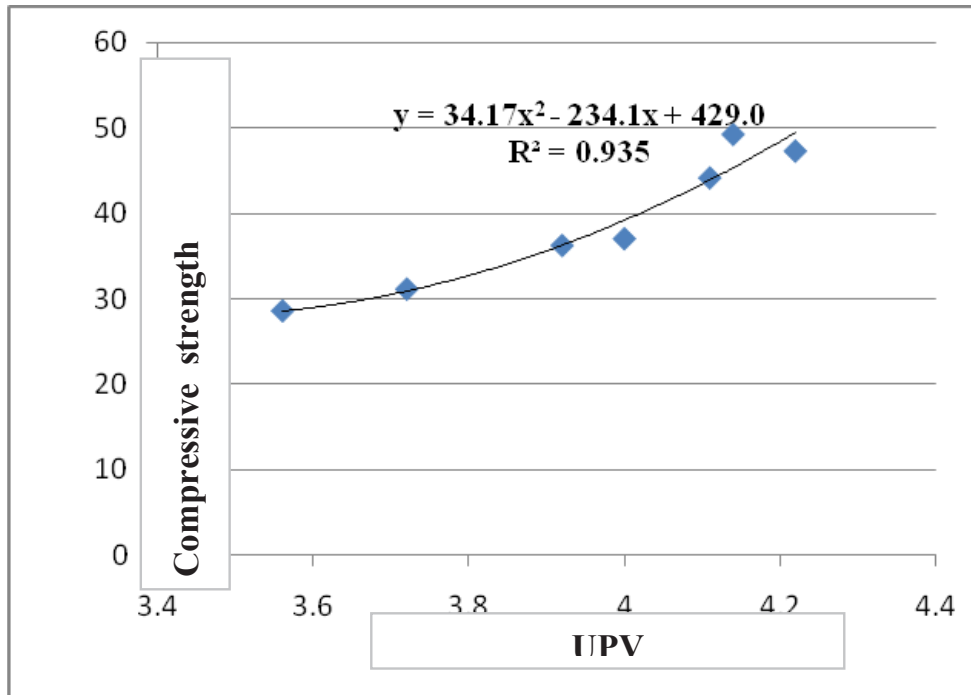$$y = 4.069x^2 - 48.95x + 177.6$$
$$R^2 = 0.889$$

Flexural strength

Compressive strength
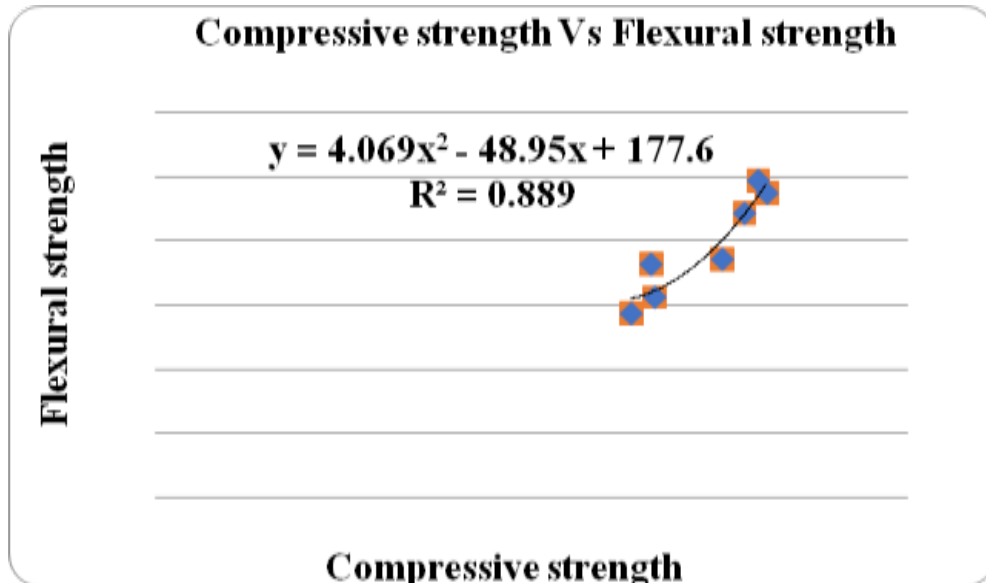
Figure 4.25 Compressive strength Vs Flexural strength

$$y = 0.23x2 + 0.481x + 25.571$$
$$R^2 = 0.836$$

Compressive strength

Rebound Hammer

Figure 4.26 Compressive strength Vs Rebound hammer

$$y = 34.17x^2 - 234.1x + 429.0$$
$$R^2 = 0.935$$

Figure 4.27 Compressive strength Vs UPV

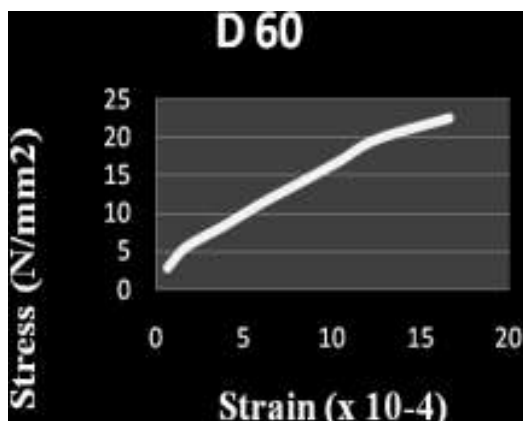**4.6   COMPRESSIVE STRESS STRAIN CHARACTERSTICS**

The compressive stress-strain characteristics were studied using cylinder specimens of size 150mm x 300mm for all mixes and are shown in Figure 4.28.
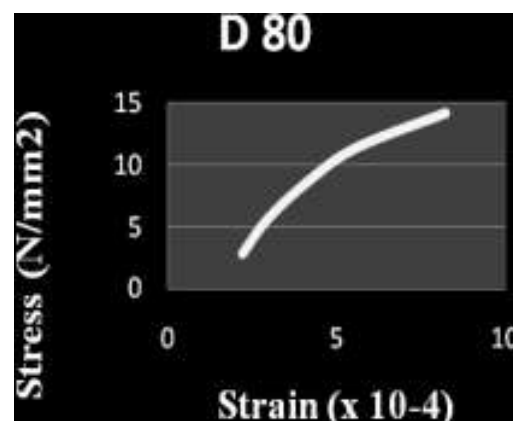

(a)

(b)

(c)

(d)

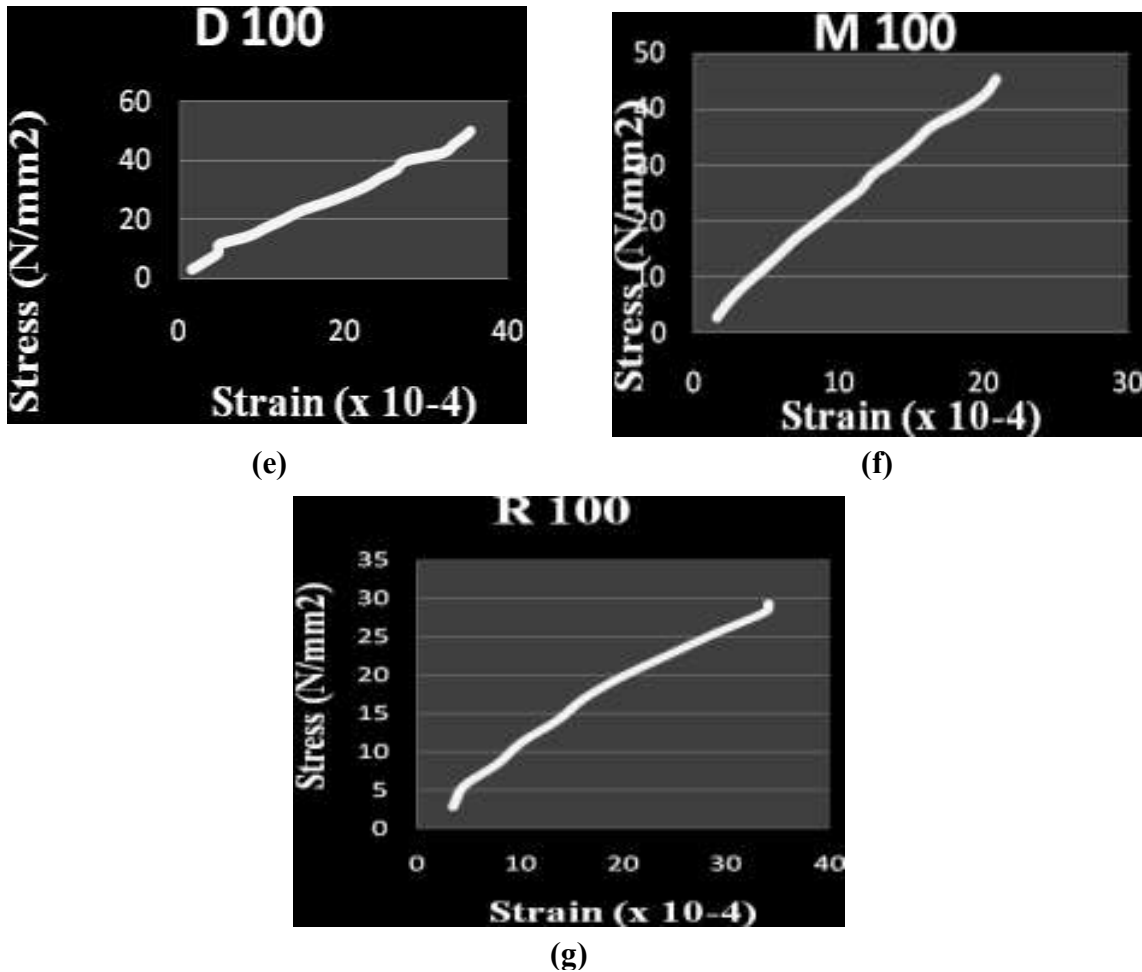**(e)**

(f)

(g)
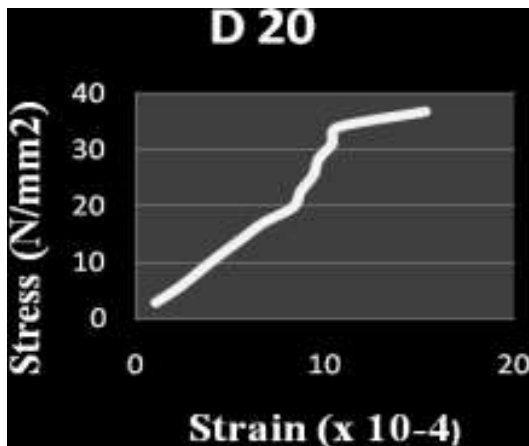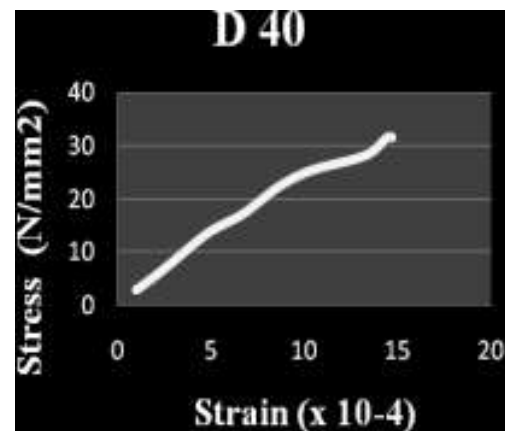
Figure 4.28 Compressive stress-strain (a) D20, (b) D40, (c) D60, (d) D80, (e) D100, (f) M100 and (g) R100
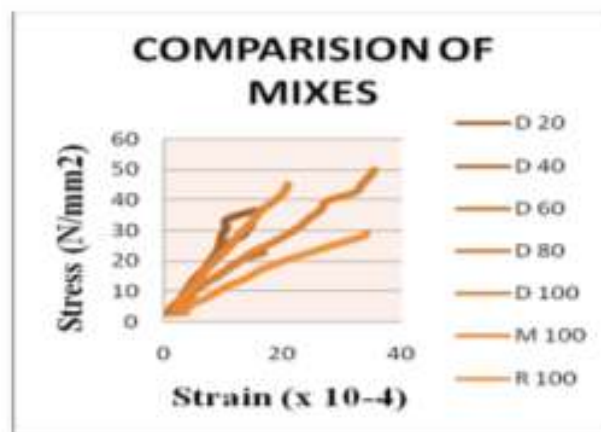

Figure 4.29 Comparison graph of all mixes

From the plots on compressive stress-strain (Figure.4.28 and Figure 4.29), it shall be observed that the variation is initially linear and remains elastic upto maximum compressive strength (0.45 fc).The elasticity of modulus was found out using the slope of the stress strain curve and noticed to increase with the strength of concrete.

In general, geopolymer concrete is brittle in nature and also the plots confirmed the same. After the peak point, the strain has dropped suddenly and as such it

was not able to get the post peak behaviour. The variation of compressive stress-strain is almost similar for all mixes.

In this investigation also, D100 proves to be good among DMS samples. With regard to control specimens, behaviour of R100 is good. The compressive stress-strain behaviour also yields the same pattern as that from flexural strength of concrete.

5. Conclusions

a. D100 beam is carrying a ultimate load of only 3.26% lesser than R100 beam and 2.51% lesser than M100 beam. However, achieves the target strength.

b. Deflection of D100 beam is 13.32% more than R100 beam while 25.32% more than M100 beam. However well within the limits.

c. Performance of D100 beam is not good in case of cyclic loading and hence not recommended for structures subjected to cyclic loading.

d. It is concluded from the rebound hammer test that 100% DMS gives good strength and if at all combination is made 20:80 (DMS: M-Sand) and vice versa shall be recommended.

e. The maximum pulse velocity obtained in case of D100 reflects well packed condition.

f. Non-destructive tests very well support the conclusions drawn from destructive tests.

g. Regression analysis indicates that no much difference between experimental and estimated values.

REFERENCES

1. Aaron Paul Wilson Procedia Engineering, vol**. 4**, pp. 1-5.
2. Anuradha, R, Sreevidya, V &Venkatasubramani, R 2013, Asian Journal of Chemistry, vol. **25**, pp. 1095-1097.
3. Arora, NK 2016, American Journal of Engineering research (AJER), vol. **5**, pp. 2438-2444.
4. Askarian, M, Zhong Tao, Georgius Adam &BijanSamali 2018, Construction and Building Materials.ElsevierLtd,vol.**186**, pp. 330-337.
5. Babaee, M & Castel, A 2016, 'Cement and concrete research chloride-induced corrosion of reinforcement in low-calcium fly ash-based geopolymer concrete', Cement and Concrete Research, Elsevier Ltd, vol. **88**, pp. 96-107.
6. Chu S.H and Yao J.J, 2020, ' A strength model for concrete with marine dredged sediment', Journal of Cleaner Production, Elsevier Ltd, Vol.**274**, 122673

7. Chuah, S, Duan, WH, Pan, Z, Hunter, E, Korayem, AH, Zhao, XL, Collins, F &Sanjayan, JG 2016, Materials and Design. Elsevier BV, vol. **92**, pp. 571-578.

8. Claudio F, IlariaCapassoet. al 2019, Journal of Cleaner Production, Elsevier Ltd, Vol.**229,** pp.1-9

9. Dashtisara 2015, Thesis and Dissertations pp. 1-49.

10. Dave, N, Anil Kumar Mishra, AmitSrivatsava, S &Koushik, K 2016, International Journal of Sustainable Built Environment, The Gulf Organisation for Research and Development, vol. **6**, pp. 30-36.

11. Davidovits, J 1994, First Internatonal Conference Proceedings on Alkaline Cement and Concretes, pp. 131-149

12. Ding, Y, Shi, C & Li, N 2018, Construction and Building Materials, vol. **190**, pp. 787-795.

13. Embong, R, AndriKushibiantoro, NasirShafiq&Muhdfadhilnurrudi 2015, 'Journal of Cleaner Production, Elsevier Ltd, vol. **112**, pp. 816-822.

14. Ganesan, N, Abraham, R & Raj, SD 2015, Construction & Building Materials, Elsevier Ltd, vol**. 93**, pp. 47-476.

15. HoussamSlimanou, KarimaBouguermouh and NedjimaBouzidi 2019, Materials Letters, Elsevier Ltd, Vol.**251**, pp 188-191

16. Isamu Yoshitake, Hiroaki Hasegawa et al. 2020, 'Engineering Structures, Elsevier Ltd, Vol. **206**, 110175.

17. Islam, A, Johnson Alengaram, U, MohdZamminJummat, NurrashquinBintiGhazali, SummiyaniYusoff&IfteekhairIbnulBhasar 2017, Construction and Building Materials, Elsevier Ltd, vol. **152,** pp. 964-977.

18. Janani, R &Revathi, A 2015, International Journal of Science, Engineering and technology Research (IJSETR), vol. **4**, pp. 1054-1057.

19. Juntao Dang, Hongjian Du and Sze Dai Pang ,2020, JussaraLimeir, Luis Agullo& Mirren Exteberria 2012, 'Dredged marine sand as construction material', European Journal of Environmental and Civil Engineering, vol. **16**, pp. 37-41.

20. Kaur, M, Singh, J &Kaur, M 2017, Ceramics International. vol. **44,** pp. 1534-1537.

21. Kupwade-patil, K &Erez N Allouche2013, Journals of Materials in Civil Engineering, ASCE, vol**. 25**, pp. 1465-1476.

22. Li, S 2018, Construction and Building Materials, Elsevier Ltd, vol. **163**, pp. 668-680.

23. Li, X, Xinwei Ma, Shoujie Zhang &EnzuZheng2013, Materials, pp. 1485-1495.

24. Limeira, J, Agullo, M, Etxeberria, M &Mollin, D 2011Construction and Building Materials, Elsevier Ltd, vol. **25**, pp. 4165-4174.

25. Limeira, J, Agullo, L &Etxeberria, M 2010, Construction and Building Materials, Elsevier Ltd, vol. **24**, pp. 863-870.

26. Lirer, S, Liguori, B, Cappaso, I, Flora, A &Caputa, D 2017, Journal of Environmental Management, Elsevier Ltd, vol. **191**, pp. 1-7.